Improvement in Thermal Resistance of Surface-Emitting Quantum Cascade Laser by Using a Diamond Submount

Shigeyuki Takagi[1], Hirotaka Tanimura[1] [a] , Tsutomu Kakuno[2], Rei Hashimoto[2],
Kei Kaneko[2] and Shinji Saito[2] [b]

[1]Department of Electrical and Electronics Engineering, School of Engineering, Tokyo University of Technology,
1404-1 Katakura, Hachioji, Tokyo, Japan
[2]Corporate Manufacturing Engineering Center, Toshiba Corporation, 33 Shinisogo, Isogo, Yokohama, Kanagawa, Japan

Keywords: Quantum Cascade Lasers, QCLs, Surface-Emitting QCL, Photonic Crystal, PhC, Static Method, Structure Function, Thermal Resistance, Thermal Flow Analysis, Diamond Submount.

Abstract: To reduce thermal resistance and improve heat dissipation in surface-emitting quantum cascade lasers (QCLs), we investigated their structure in which a diamond submount is inserted between a mesa and a CuW mount. From the results of the thermal flow simulation of three-dimensional models of the QCLs, the thermal resistance of the QCL without the diamond submount was 8.5 K/Wand that of the QCL with the diamond submount was 5.2 K/W. From the structure function obtained using the static method, the thermal resistance of the QCL without the diamond submount was 8.5 K/W and that of the QCL with the diamond submount was 6.3 K/W. From the measured output range of the QCLs, the measurement output power of the QCL without the diamond submount was 265 mW and that of the QCL with the diamond submount was 290 mW. The reduction in thermal resistance and the improvement in laser output were confirmed to be due to the diamond submount.

1 INTRODUCTION

A quantum cascade laser (QCL) is an n-type semiconductor laser that emits light in the infrared region (Faist et al., 1994). Since its emission wavelength is in the infrared region called the molecular fingerprint region, the QCL can measure many gases with high sensitivity. From its merits, it is expected to be applicable to the detection of trace substances and distant gases. In the detection of trace substances, the amount of laser light absorbed is measured and a long optical path is necessary for laser light propagation. In the detection of distant gases, a high-output laser is required because the reflected light is detected during laser light propagation.

Evans et al. have developed a watt-order laser oscillation as a high-power laser (Evans et al., 2007). This laser is an edge-emitting device in which the direction of the laser light excitation coincides with that of laser light emission. In contrast, a surface-emitting QCL that emits laser light from the surface

in the vertical direction of the device through a photonic crystal (PhC) was previously developed (Colombelli et al., 2003). By widening the area of the excitation part called the mesa, we can expect improvements in beam quality and heat dissipation.

In our previous study, we developed surface-emitting QCLs and confirmed single-mode laser oscillations (Saito et al., 2021, Yoa et al., 2022). In addition, to evaluate the heat dissipation of these QCLs, we measured their thermal resistance using the structure function (Takagi et al., 2019). Furthermore, we constructed a three-dimensional (3D) thermal flow simulation model and evaluated the thermal resistance of these surface-emitting QCLs (Takagi et al., 2022)

In our current study, we have developed a prototype of a surface-emitting QCL with a diamond submount and demonstrated the reduction in thermal resistance quantitatively. We report these results and the improvement in laser output.

[a] https://orcid.org/0000-0002-7653-4602
[b] https://orcid.org/0000-0002-1829-6482

2 3D THERMAL FLOW SIMULATION OF SURFACE- EMITTING QCL

2.1 Surface-Emitting QCL

Figure 1 shows the structure of the surface-emitting QCL in which (a) is a cross-sectional view, (b) is a view from above, and (c) is a bottom view. A mesa that emits laser light and a dummy ridge were formed on an InP substrate with a thickness of 600 μm. In the mesa area, an InP film was formed on an active layer (laser excitation portion) that excites a laser, and a photonic crystal was formed on the InP film. Au electrodes for current supply was formed on the opposite side of the InP substrate. A CuW mount was mounted on the mesa and dummy ridge sides of the InP substrate, resulting an epi–side–down structure.
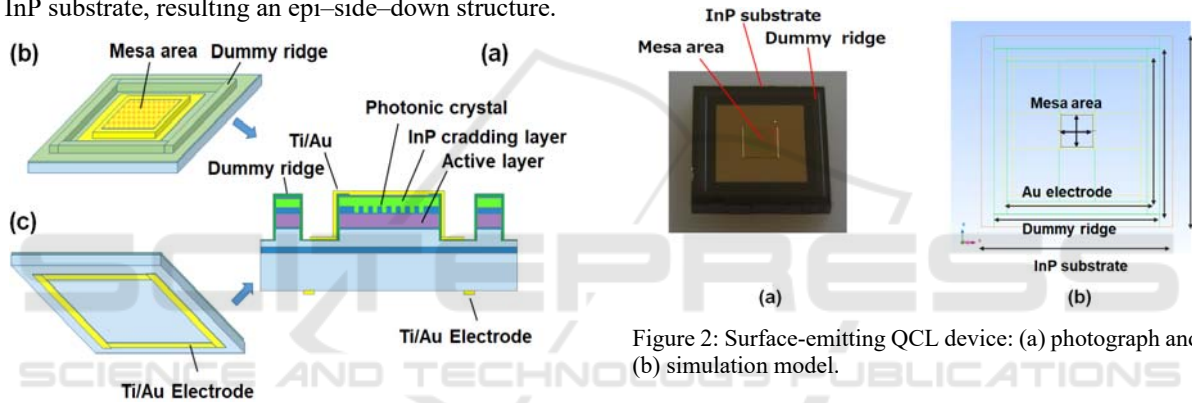

Figure 1: Surface-emitting QCL. (a) Cross-sectional view, (b) top view, and (c) bottom view.

2.2 3D Simulation Model

A simulation model was constructed by inputting the 3D structure and physical property data of the surface-emitting QCL. The thermal flow analysis software STEAM (MSC software) was used as the simulator. The analysis is based on a natural convection model, in which the laser excitation portion is overheated and natural convection occurs (Ho et al., 2008). The equation for gas flow is

$$\frac{\partial \rho}{\partial t} + \frac{\partial(\rho v_x)}{\partial x} + \frac{\partial(\rho v_y)}{\partial y} + \frac{\partial(\rho v_z)}{\partial z} = 0 , \quad (1)$$

where ρ is the density and t is the time. v_x, v_y, and v_z are the velocities in the x, y, and z directions, respectively. Moreover, the formula for heat transfer is

$$\frac{\partial u}{\partial t} = \frac{K}{\sigma \rho} \left(\frac{\partial^2 u}{\partial x^2} + \frac{\partial^2 u}{\partial y^2} + \frac{\partial^2 u}{\partial z^2} \right) + \frac{1}{\sigma} F(x, y, z, t) , \quad (2)$$

where u is the temperature, which is a function of the position and time, σ is the specific heat, K is the thermal conductivity, and F is the external heating value per unit time, which is a function of the position and time.

Figure 2(a) shows a photograph of the surface-emitting QCL prototype fabricated on the basis on the design in Fig. 1. Corresponding to Fig. 1(b), it can be observed that a mesa and a dummy ridge are formed on the InP substrate. Figure 2(b) is a simulation model of the QCL on an InP substrate, showing the outline of the InP substrate, mesa, dummy ridge, and Au electrodes on the back surface.

Figure 2: Surface-emitting QCL device: (a) photograph and (b) simulation model.

The InP substrate in Fig. 2(a) was mounted on a CuW mount with an epi–side–down structure. Figure 3(a) shows a 3D model of the QCL on a CuW mount without a diamond submount. Figure 3(b) shows 3D model of the QCL mounted with a diamond submount. Diamond has a high thermal conductivity and was reported to reduce thermal resistance in light emitting devices (Bezotosnyi et al., 2014). In the simulation model, the diamond submount was placed on the CuW mount and The InP substrate was placed on the diamond submount with an epi–side–down structure. The thermal conductivity of the diamond submount was set at 2000 W/mK.

Other physical property values in this 3D model are as follows. The thermal conductivities of the CuW mount, InP, SiO$_2$, Ti, Au, and Cu was 157 W/mK, 68 W/mK, 1.38 W/mK, 21 W/mK, 296 W/mK, and 403 W/mK, respectively. The thermal conductivity of the Au-buried PhC part was determined from the volume ratio of photonic crystal and InP cradding. In the laser pumping part, Al$_{0.638}$In$_{0.362}$As and Ga$_{0.331}$In$_{0.669}$As thin films were alternately laminated. From the

83

references, the thermal conductivity of $Al_{0.638}In_{0.362}As$ thin film was 10.0 W/mK (Kim et al., 2002), and that of the $Ga_{0.331}In_{0.669}As$ thin film was 5.6 W/mK (Adachi, 1985). From the film thicknesses of both thin films, the thermal conductivity of the laminated thin film was calculated to be 7.5 W/mK. Regarding the temperature boundary conditions, the temperature of Peltier cooler was fixed at 0°C at the mount, and the ambient temperature of the surface-emitting QCL is set at 30°C. The temperature increase was calculated assuming that the power from the power source is supplied to the laser pumping section.
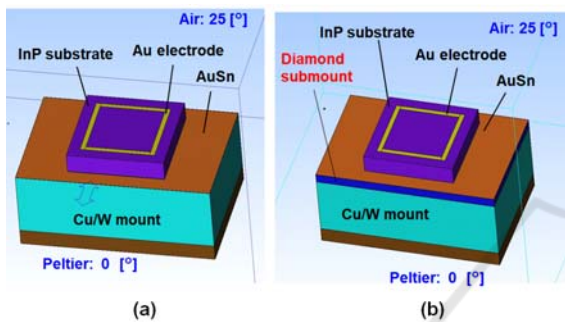

Figure 3: 3D model for thermal flow simulation. (a) QCL without diamond submount and (b) QCL with diamond submount.

2.3 Simulation Results

The temperature distribution of the surface-emitting QCL was calculated with an input power of 10 W to the laser excitation portion. Figure 4(a) shows the temperature distribution of the QCL without a diamond submount, and Fig. 4(b) shows that of the QCL with the diamond submount. The temperature distribution in the central cross section of the surface-emitting QCL is also shown. The temperature of the Peltier cooler was fixed at 0°C, and that of the CuW mount was also near 0°C owing to its high thermal conductivity. The temperature is high in the laser excitation portion where the power was supplied and the portion in the mesa around the excitation portion. The temperature increase at an input power of 10 W was determined to be 82.63°C in the QCL without a diamond submount and 52.47 °C in the QCL with a diamond submount. The temperature increase was suppressed by using the diamond submount.

In Fig. 4(a), the isotherms under the mesa are semi-circular, and heat is concentrically transmitted around the mesa. On the other hand, in Fig.4(b), owing to the high thermal conductivity of the diamond submount, the heat spreads horizontally and is transmitted vertically through the CuW mount. To

investigate the thermal flow in more detail, we calculated the heat flux of the surface-emitting QCL. Figure 5(a) shows the distribution of thermal flux vectors of the QCL without a diamond submount, and Fig. 5(b) shows that of thermal flux vectors of the QCL with a submount. In Fig.5(a), the heat is mainly directed from the mesa, while in Fig 5(b), a horizontal thermal flux vector is generated in the diamond submount. From the temperature distribution in Fig. 4 and the thermal flux distribution in Fig. 5, we consider that heat is transmitted horizontally by the diamond submount, thereby reducing the thermal resistance.
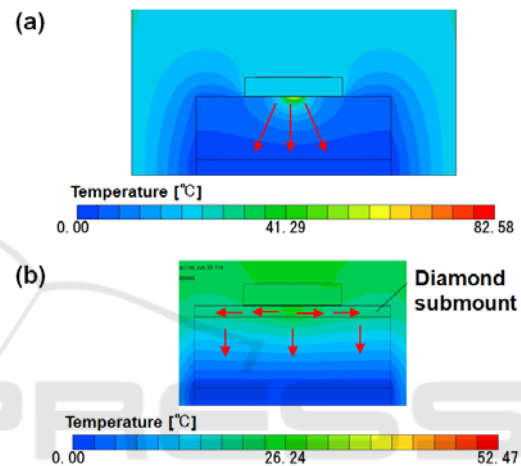

Figure 4: Simulation results of temperature distributions. (a) QCL without diamond submount and (b) QCL with diamond submount.
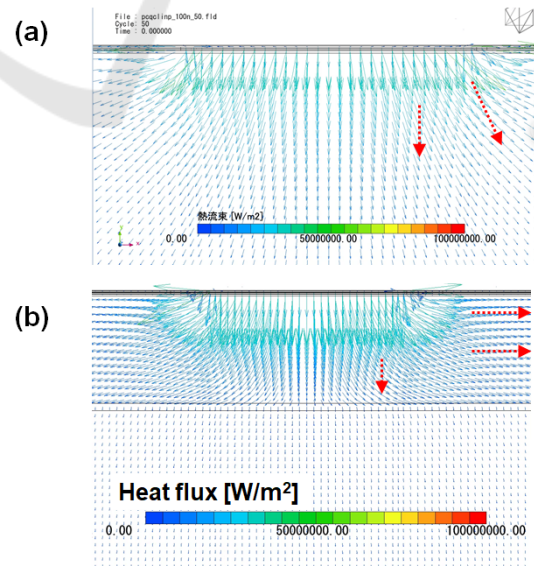

Figure 5: Simulation results of heat flux. (a) QCL without diamond submount and (b) QCLwith diamond submount.

Next, we calculated the temperature increase with respect to the input power. The obtained results are shown in Fig.6. The temperature increases at 10 W show a thermal resistance of 8.26 K/W in the QCL without a diamond submount and a temperature resistance of 5.25 K/W in the QCL with a diamond submount. As the input power increases, the temperature difference between the QCLs with and without a diamond submount increases. This shows that the diamond submount is more effective under high input power operating conditions.
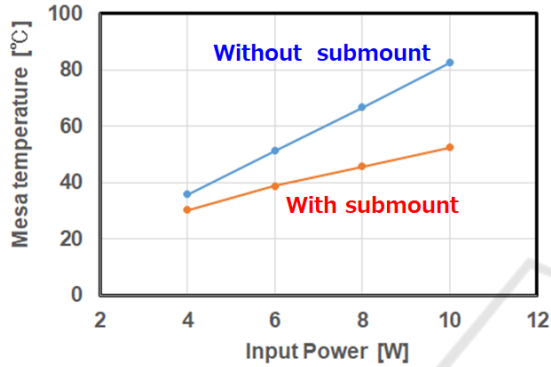

Figure 6: Relationship between input power and mesa temperature.

3 THERMAL RESISTANCE MEASUREMENTS OF SURFACE-EMITTING QCLS

3.1 Static Method and Structure Function

In this study, a statics method was applied to the thermal resistance measurements of the surface-emitting QCLs. In the statics method, after heating devices, thermal resistance is measured from the voltage–current characteristics obtained during cooling. The measurement method has short measurement time and high reproducibility. T3Ster (Siemens AG) was used for the measurement. Since the resistance of a semiconductor device changes with temperature, the temperature change is proportional to the voltage change across the device when a constant current is allowed to flow. In the statics method, this voltage change ΔT_{SP} [mV] is measured and the temperature change ΔT_j [K] of the device is obtained as (Székely, 1997)

$$\Delta T_j = K \cdot \Delta T_{SP}, \tag{3}$$

where K is a coefficient called the K-factor. A surface-emitting QCL was set in the thermostat of T3Ster, and the K-factor was measured by changing the thermostat temperature from 20℃ to 70℃. As a result, the K-factor was determined as –0.022772. K/V.

T3Ster was used to measure the structure function by the statics method. The CuW mount was cooled to 20°C and heated by supplying approximately 1.6 W of power to the QCL. After stopping the heating power supply, the temperature of the QCL during cooling was measured to obtain a cooling curve. Assuming that the thermal resistance and thermal capacity of the elements constituting the QCL are R_{th} and C_{th}, respectively, the time constant τ during cooling is expressed as

$$\tau = C_{th} \cdot R_{th}. \tag{4}$$

3.2 Measurement Results

Surface-emitting QCLs of the same lot were mounted with and without a diamond submount. Figures 7(a) and (b) show the QCL mounted without a diamond submount and the QCL mounted with a diamond submount, respectively. The CuW mount and surface-emitting QCL were soldered to the diamond submount with indium.
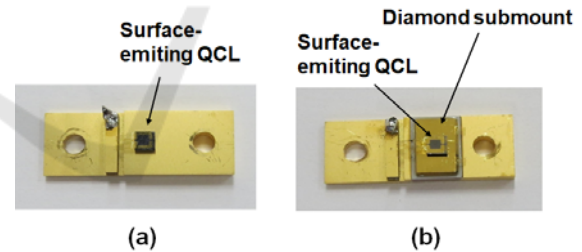

Figure 7: Photographs of the mounted surface-emitting QCLs: (a) without and (b) with diamond submount.

Figures 8(a) and (b) show the cooling curves of the QCLs without diamond submount and with the diamond submount measured by the static method, respectively. Figures 9(a) and (b) show the structure functions of the QCLs without and with the diamond submount obtained from the cooling curves shown in Fig. 8, respectively. In the flat area above 8.5 K/W in (a), the thermal resistance value fluctuates when the mounting method of the surface-emitting QCL is changed during measurement. Therefore, the thermal resistance

over of the flat region was considered to be the thermal resistance between the surface-emitting QCL and the T3Ster cooler. We estimated a typical value of 8.5 K/W for the total thermal resistance of surface-emitting QCLs. Similarly, the thermal resistance of the QCL in (b) was estimated to be 6.3 K/W.
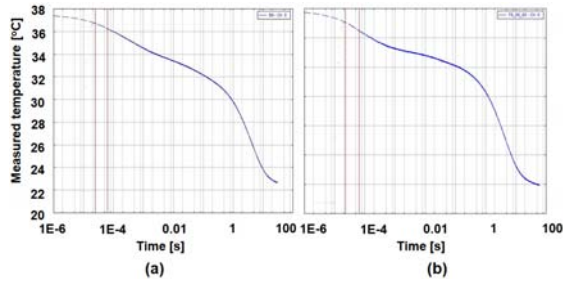

Figure 8: Cooling curves of QCLs (a) without and (b) with diamond submount.
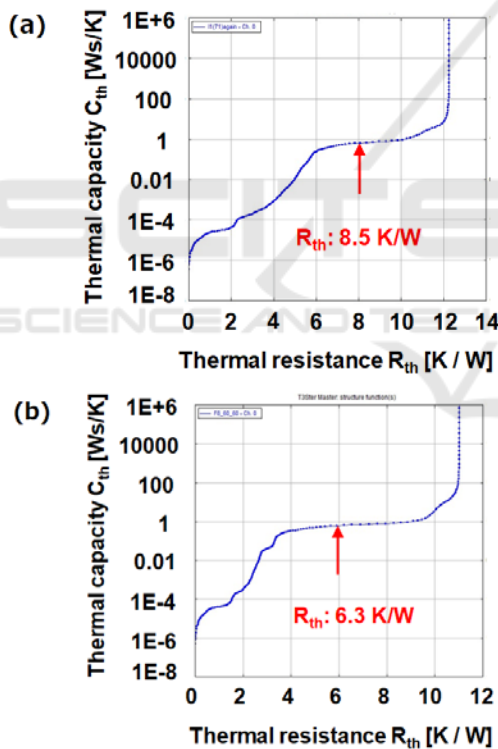

Figure 9: Structure functions of QCLs (a) without and with diamond submount (b).

4 LASER OSCILLATION

To investigate the effect of the diamond submount, the laser power was measured. The QCL operating conditions were a frequency of 100 KHz, a duty of

1%, and a cooling temperature of 77 K. Figure 10 shows the measurement results. Although increases with the supply current, the laser output stops increasing at around 12 A for the QCL without a diamond submount. In contrast, the QCL with a diamond submount increases in the output even at a current of 17 A. The maximum output power within the measured range was determined 265 mW for the QCL without a diamond submount and 290 mW for the QCL with a diamond submount. This indicates that the diamond submount improved the heat dissipation and output of the QCL.
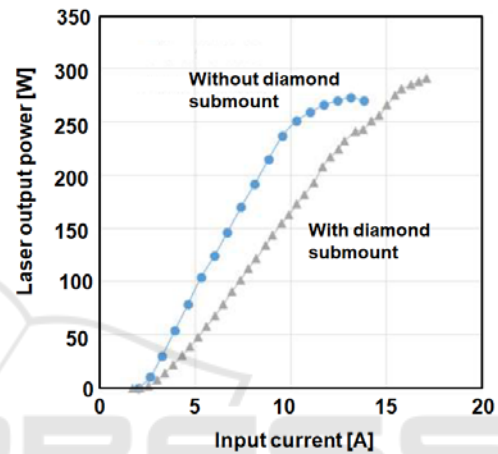

Figure 10: Output powers of QCLs without and with diamond submount.

5 CONCLUSIONS

To reduce thermal resistance and improve heat dissipation in surface-emitting QCLs, we investigated their structure in which a diamond submount is inserted between a mesa and a CuW mount. From the thermal flow simulation of 3D models of the QCLs, the thermal resistance of the QCL without the diamond submunt was 8.5 K/W and that of the QCL with the diamond submount was 5.2 K/W. From the structure function obtained using the static method, the thermal resistance of the QCL without the diamond submount was 8.5 K/W and that of the QCL with the diamond submount was 6.3 K/W. The simulation results and structure function of the QCL with the diamond submount show that the reduction in thermal resistance is caused by the diamond submount. From the measured output range of the QCLs, the maximum output power of the QCL without the diamond submounit was 265 mW and that of the QCL with the diamond submount was 290 mW. The reduction in thermal resistance and the

improvement in laser output were confirmed to be due to the diamond submount.

ACKNOWLEDGEMENTS

REFERENCES

Faist, J., Capasso, F., Sivco, D. L., Sirtori, C., Hutchinson, A., & Cho, A. Y. (1994). Quantum cascade laser. *Science*, 264, 553–556.

Evans, A., Darvish, S. R., Slivken, S., Nguyen, J., Bai, Y., & Razeghi, M. (2007). Buried heterostructure quantum cascade lasers with high continuous-wave wall plug efficiency. *Appl. Phys. Lett.*, 91, 071101-1–3.

Colombelli, R., Srinivasan, K., Troccoli, M., Painter, O., Gmachl, C. F., Tennant, D. F., Sergent, A. M., Sivco, D. L., Cho, A. Y., & Capasso, F. (2003). Quantum cascade surface-emitting photonic crystal laser. *Science*, 302, 1374–1377.

Saito, S., Hashimoto, R., Kaneko, K., Kakuno, T., Yao, Y., Ikeda, N., Sugimoto, Y., Mano, Y., Kuroda, T., Tanimura, H., Takagi, S., & Sakoda, K. (2021). Design and fabrication of photonic crystal resonators for single-mode and vertical surface emission from strain-compensated quantum cascade lasers operating at 4.32 μm. *Appl. Phys. Express*, 14, 102003-1–5.

Yao, Y., Ikeda, N., Chalimah, S., Kuroda, T., Sugimoto, Y., Mano, T., Koyama, H., Hashimoto, R., Kaneko, K., Kakuno, T., Ookuma, S., Togawa, T., Ohno, H., Saito, S., Takahashi, H., Tanimura, H., Takagi, S., & Sakoda, K. (2022). Improved power and far-field pattern of surface-emitting quantum cascade lasers with strain compensation to operate at 4.3 μm", *Jpn. J. Appl. Phys.* 61, 052001-1–8.

Takagi, S., Tanimura, H., Kakuno, T., Hashimoto, & R., Saito, S. (2019). Thermal analysis and heat dissipation improvement for quantum cascade lasers through experiments, simulations, and structure function. *Jpn. J. Appl. Phys.*, 58, 091008-1–6.

Takagi, S., Tanimura, H., Kakuno, T., Hashimoto, R., Saito, S. (2022). Improvement of thermal resistance of surface-emitting quantum cascade laser using structural function and 3D thermal flow simulation. *10th International Conference on Photonics, Optics, and Laser Technology*, 128–132.

Ho, C. J., Chen, M. W., & Li, Z. W. (2008). Numerical simulation of natural convection of nanofluid in a square enclosure: Effects due to uncertainties of viscosity and thermal conductivity, *Int. J. Heat Mass Transfer*, 51, 4506–4516.

Bezotosnyi, V. V., Krokhin, O. N., Oleshchenko, V. N., Pevtsov, V.A., Popov, Y. M., & Cheshev, E. A. (2014). Thermal modelling of high-power laser diodes mounted using various types of submount. *IEEE J. Quantum Electron.*, 44, 899–902.

Kim, Y. M., Rodwell, M. J. W., & Gossard, A. C. (2002). Thermal characteristics of InP, InAlAs, and AlGaAsSb metamorphic buffer layers used in $In_{0.52}Al_{0.48}$/$In_{0.53}Ga_{0.47}As$ heterojunction bipolar transistors grown on GaAs substrates. *J. Electron. Mater.*, 31, 196–199.

Adachi, S. (1985). GaAs, AlAs, and AlxGa1−xAs: Material parameters for use in research and device applications. *J. Appl. Phys.*, 58, R1–R29.

Székely, V. (1997). A new evaluation method of thermal transient measurement results. *Microelectron. J.*, 28, 277–292.